Ultrastructural Organization of Blood-C-Cell Interrelationships in Thyroid Gland Guanethidine-Desympathized Four-Week-Old Rats

R. A. Krasnoperov, S. V. Grachev, V. A. Glumova, S. N. Ryashchikov, and S. I. Volkova

Translated from *Byulleten' Eksperimental'noi Biologii i Meditsiny*, Vol. 122, No. 12, pp. 678-681, December, 1996
Original article submitted March 22, 1995

Morphometry of electron microscopic preparations reveals a compensatory and adaptive nature of ultrastructural changes in the thyroid blood-C-cell junctions induced by desympathization. The data suggest the involvement of adrenergic innervation in neurohumoral regulation of the blood-C-cell relationships in the thyroid gland.

Key Words: *desympathization; guanethidine monosulfate; blood-cell barrier; thyroid gland*

Previous investigations have demonstrated a strong dependence of the C-cell apparatus of the thyroid gland (TG) on sympathetic innervation [3,8,10,14]. The abundant morphological substrate for adrenergic innervation in the thyroid parafollicular epithelium and in blood capillaries adjacent to the basal pole of C-cells [2,7,13] implies the importance of catecholaminergic stimulation for optimal blood-C-cell (BCC) interactions in the TG. However, this problem remains little explored, which hampers the formulation of a morphofunctional concept of the BCC functioning.

The aim of the present study was to describe the ultrastructural organization of BCC interactions in the TG of desympathized animals.

MATERIALS AND METHODS

Random-bred male albino rats (n=17) were injected subcutaneously with a guanethidine solution (Pliva) in a dose of 15 mg/kg/day from day 0 to day 14 after birth. This led to intense degradation of intrathyroid adrenergic fibers [7,8] and elimination of more than 75% of the neurons in the superior cervical sympathetic ganglion, which is the sole source of catecholaminergic innervation of rat TG [15]. Control rats (n=18) were injected with the same volume of isotonic NaCl solution.

The desympathized and intact 4-week-old animals were decapitated after ether vapor overdosage. The fragments of TG were incubated in 3% glutaraldehyde and 1% osmium tetroxide in phosphate-buffered saline (pH 7.4), dehydrated, and embedded in Epon-Araldyte. Ultrathin sections were cut with an LKB III microtome, contrasted by the method of Reynolds and examined under a JEM-100B electron microscope.

The parameters of BCC junctions were analyzed morphometrically on negatives, electromicrograms, and on the microscope screen using a built-in binocular lens. The length of the vascular (basal) pole of calcitoninocyte was determined using the random secant method. The parameters of paravasal interstitium, juxta-C-cell (JCC) fragment of endotheliocyte, basement membranes of thyroid adenomere, and perifollicular hemocapillary were calculated from the formula of the mean thickness of the layer with some modifications [1]. Transmural transport in the

Laboratory of Extreme States, Research Center of I. M. Sechenov Medical Academy, Moscow; Department of Biology, Izhevsk Medical Institute; Republic Cardiology Dispensary, Izhevsk

0007-4888/96/0012-1236$15.00

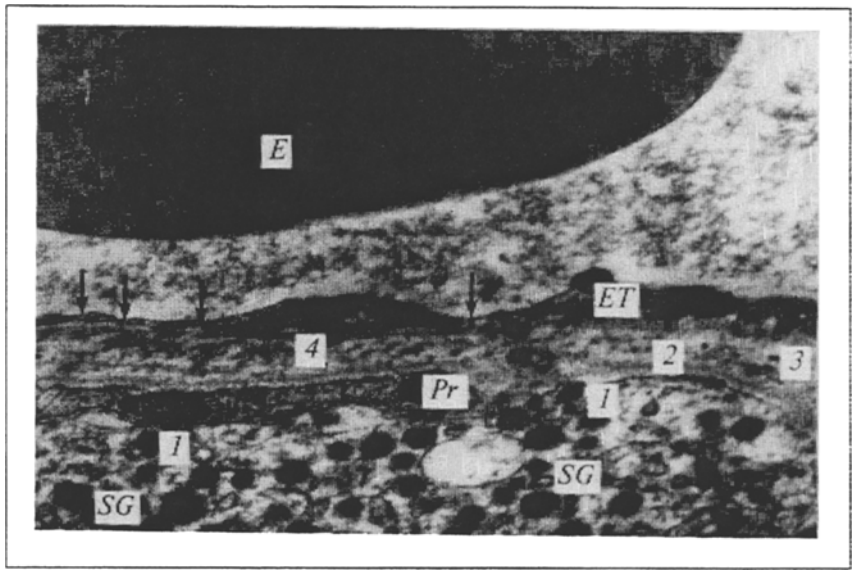

Fig. 1. Ultrastructural organization of BCC junction in TG of a desympathized rat. The following components of the BCC complex are seen: plasmalemma of the vessel pole of a C cell (*1*), basement membrane of a follicle (*2*), pericapillary interstitium (*3*), basal lamina of a JCC hemocapillary (*4*), basement surface, cytoplasm, and luminal surface of an endotheliocyte. Here and in Fig. 2: *E*: erythrocyte, *SG*: secretory granules; *Pr*: cytoplasmic process of C cell; *ET*: endotheliocyte. Fenestrations are indicated by arrows. ×12,800.

JCC zone of an endotheliocyte was assessed by the mean number of fenestrations and plasmalemmal microvesicles (the total number, and basal, luminal, and cytoplasmic fractions) on cross section of a hemocapillary. The diameters of specialized transendothelial transporting organelles were measured using built-in ocular planimetric grid. The area of the lumen of a JCC-microvessel was assessed by point count.

The absolute parameters of BCC junctions were calculated using the corresponding coefficients [4]. In order to compensate for distortion arising when the plane of ultrathin sections is not perpendicular to the longitudinal axis of the JCC-fragment of a perifollicular capillary, all necessary measurements in the zone of BCC coupling were performed assuming that $B/L \geq 0.9$ (i.e., $CV < 0.5\%$), where B and L are the small and the large axes of the microvessel, its basal surface being approximated to a cylinder. The above-mentioned coefficient of variation (CV) provides the accuracy of morphometrical analysis of BCC coupling zone which is comparable with that provided by radioimmune assays [11,12]. The data are presented as $\bar{X} \pm s_{\bar{x}}$. The significance of differences was evaluated using Student's t test after the distribution of the test parameter had been proven to be normal by the asymmetry coefficient.

RESULTS

Under conditions of subtotal adrenergic denervation the BCC interactions in the thyroid gland retained the typology of ultrastructural elements observed in intact animals [6] (Fig. 1), irrespective of statistically significant changes in the size of some components of the BCC complex. Of particular interest are the significant changes in the mean length of the vascular pole of C cells (Table 1). This phenomenon indicates a reduction in the effective area of the BCC barrier and is consistent with the observation that the disorders in the architectonics of sympathetic terminals in the TG of young rats [8] decreased the incretory activity of parafollicular epitheliocytes.

Accelerated involution in the adrenergic portion of the autonomic nervous system also affects spatial

TABLE 1. Ultrastructural Parameters of BCC Complexes in the TG of Desympathized and Intact Rats

Parameter	Group	
	experiment	control
Length of vessel pole of C cell, μ	9.4±0.18*	13.4±0.22
Mean thickness of basement membrane of thyroid follicle, nm	61.4±2.03	59.5±1.55
Mean thickness of pericapillary interstice, nm	478±8.7*	426±9.3
Mean thickness of basal lamina of JCC hemocapillary, nm	85.8±3.78	82.2±3.38
Mean thickness of C cell adjacent peripheral zone of endotheliocyte, nm	170±17	184±20
Lumen of JCC fragment of perifollicular capillary, μ^2	32.4±2.35*	19.8±1.49

Note. *$p<0.001$ compared with the control.

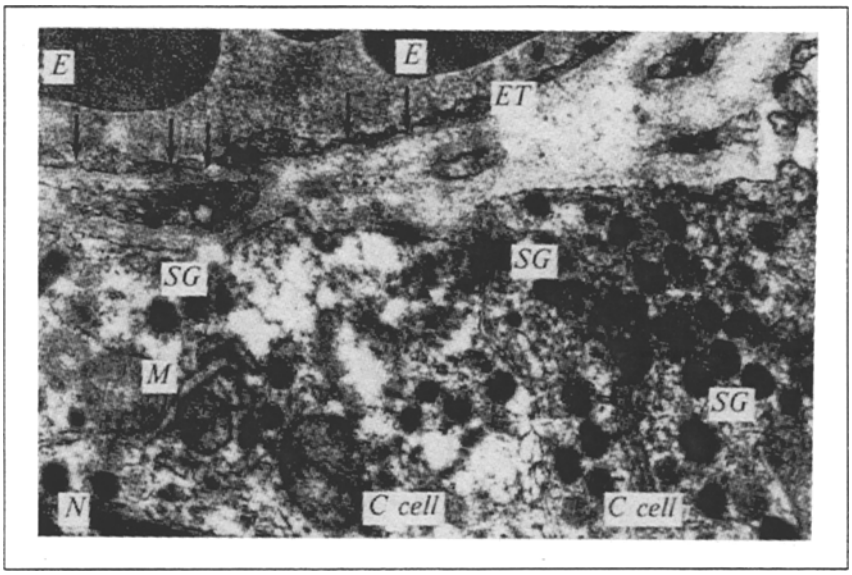

Fig. 2. A rare form of BCC complex. Vessel poles of two C cells (C cell) are juxtaposed to the fenestrated (peripheral) zone of a JCC endotheliocyte. *M*: mitochondrion; *N*: nucleus of a C cell. Desympathized animal. ×12,000.

organization of thyroid C cell and perifollicular hemocapillary. In control rats, each JCC microvessel fragment contacts with one C cell. In desympathized rats, two C cells participate in the BCC interactions: 1.4±0.62% zones of BCC contacts, $p<0.05$ in comparison with the control (Fig. 2). It seems interesting to compare the ultrastructural rearrangement of the BCC barrier with compensatory hyperplasia of thyroid parafollicular epithelium observed during desympathization [8]. Presumably, the proliferation of C cells compensates for the deficiency of serum calcitonin, its rate being higher than that of the angiogenesis in the TG.

Elimination of the majority of neurons in the superior cervical sympathetic ganglion markedly alters the microvascular component of the BCC system. Dilation of the JCC fragment of a hemocapillary (Table 1) and entry of the plasma into the vascular wall were accompanied by a statistically significant thickening of the paravasal interstitium. Such a separation of the elements of the BCC complex combined with shortening of the basal pole of C cell may prevent changes in the physicochemical properties of the C-cell cytoplasm under conditions of pericapillary edema.

According to modern classification, an endothelial cell can be divided into several compartments, each unequally contributing to the formation of the BCC-relationships (Table 2). The typical (first) variant of the BCC complex is spatial coupling of the vascular pole of a C cell to the peripheral zone of a JCC endotheliocyte with abundant fenestration characteristic of visceral hemocapillaries [5]. After adrenergic denervation, variations of the proportion of JCC and their mean diameters were very small (Table 3). Sometimes, the capillary component of the thyroid BCC barrier includes both the peripheral zone and the interendothelial contact (the second variant, Table 2). The occurrence of spatial coupling of a parafollicular thyrocyte and the organelle- and nucleus-containing zone of an endotheliocyte was very low (the third variant of the BCC interaction).

It should be emphasized that ultrastructural organization of BCC complex in the TG, which provide coupling of the basal pole of C cell predomi-

TABLE 2. Effect of Disturbed Intrathyroid Architectonics of Adrenergic Terminals on the Percentage of Different BCC Complex Variants

Variant	Group	
	experiment	control
1st	95.2±1.13	97.3±0.84
2nd	1.7±0.69	1.9±0.71
3rd	1.7±0.69	0.8±0.47

TABLE 3. Parameters of Specialized Transendothelial Transporting Organelles in JCC Complexes in TG of Experimental and Control Animals

Parameter	Group	
	experimental	control
Microvesicles:		
total number fractions	6.3±0.35	6.0±0.40
basal	1.6±0.28	1.7±0.20
luminal	2.8±0.28	2.1±0.32
cytoplasmic	1.8±0.26	2.3±0.30
Diameter microvesicles, nm	100±8.3	86±5.8
Number of fenestrae	17.9±0.81	16.3±0.41
Diameter of fenestrae, nm	76±4.3	70±4.0

nantly with peripheral zone of endotheliocyte (most effective transport zone) was relatively stable both in intact and desympathized rats. This feature of the BCC architectonics complies with the principle of biological utility with respect to optimization of JCC-transporting processes.

REFERENCES

1. E. R. Veibel', *Morphometry of Human Lungs* [in Russian], Moscow (1970).
2. S. Yu. Vinogradov, *Arkh. Anat.*, **93**, No. 10, 57-62 (1987).
3. G. K. Zoloev, V. F. Mordovich, and V. D. Slepushkin, *Probl. Endokrinol.*, **33**, No. 1, 60-63 (1987).
4. Ya. L. Karaganov, G. A. Alimov, and S. A. Gusev, *Trudy 2nd Mosk. Med. Institute*, No. 2, 7-26 (1976).
5. Ya. L. Karaganov, A. A. Mironov, and V. A. Mironov, in: *Atlas of Scanning Electron Microscopy of Cells, Tissues, and Organs* [in Russian], O. V. Volkova *et al.* (Eds.), Moscow (1987).
6. R. A. Krasnoperov, S. V. Grachev, V. A. Glumova, *et al.*, in: *Topical Problems of Medical Morphology* [in Russian], Izhevsk (1994), Issue 3, pp. 123-124.
7. V. N. Markov, A. S. Elkin, and Yu. V. Pogorelov, in: *Reactivity and Plasticity of Organs and Tissues in Pathology and Experiments* [in Russian], V. Ya. Glumov (Ed.), Nizhnii Novgorod (1991), pp. 61-65.
8. S. N. Ryashchikov, V. N. Markov, V. A. Glumova, *et al.*, *Byull. Eksp. Biol. Med.*, **111**, No. 6, 663-666 (1991).
9. N. N. Chuchkova, A. V. Grigor'eva, and V. N. Yarygin, *Tsitologiya*, **29**, No. 6, 662-670 (1987).
10. D. P. Cardinali, *Neuroendocr. Lett.*, **7**, No. 5, 235-240 (1985).
11. X. Z. Khawaja, A. K. Chattopadhyay, and I. C. Green, *Brain Res.*, **555**, 164-168 (1991).
12. X. Z. Khawaja, I. C. Green, J. R. Thorpe, and C. J. Bailey, *Diabetes*, **39**, No. 10, 1289-1297 (1990).
13. M. A. Lopez, R. Hevia, M. J. Anitua, *et al.*, *Bull. Assoc. Anat. (Nancy)*, **74**, No. 224, 20-21 (1990).
14. A. K. Srivastav and L. Rani, *Biol. Struct. Morphog.*, **1**, No. 3, 117-123 (1988).
15. F. Sundler, T. Grunditz, R. Hakanson, and R. Uddman, *Acta Histochem. Suppl. (Jena)*, **37**, 191-198 (1989).

Ultrastructural and Stereological Analysis of the Gastric Epithelium in Wild Muridae from Regions Exposed to Anthropogenic Pollution

G. I. Nepomnyashchikh, S. V. Aidagulova, and L. M. Nepomnyashchikh

Translated from *Byulleten' Eksperimental'noi Biologii i Meditsiny*, Vol. 122, No. 12, pp. 682-686, December, 1996
Original article submitted January 10, 1996

Ultrastructural analysis of epitheliocytes in the gastric mucosa of wild Muridae captured in three regions of the Altai with various levels of ecological pollution reveals predominance of dystrophic and atrophic changes in the surface and glandular epithelium. Stereological analysis demonstrates a universal character of structural response to a complex of anthropogenic factors.

Key Words: *radiation and anthropogenic pollution; wild rodents; gastric epithelium; ultrastructure; stereology*

An attempt has been recently made to determine threshold parameters for radiation and technogenic toxicants and to substantiate biological criteria of ecological stress [2-4,7,10]. It has been emphasized that the permissible doses of adverse ecological factors should be established on the basis of ultrastructural changes [11] with proper consideration of the role of the borderline tissues [6,8]. In this context, gastric mucosa represents a convenient model. As an entry for various xenobiotics, promptly renewing gastric epithelium may serve as an indicator of the mobility of adaptive-compensatory reactions developing at the basis of regeneration processes.

Laboratory of Ultrastructural Pathology, Institute of Regional Pathology and Pathomorphology, Siberian Division of the Russian Academy of Medical Sciences, Novosibirsk

0007-4888/96/0012-1239$15.00